Title

Intermediate filament accumulation can stabilize microtubules in Caenorhabditis elegans motor neurons

Journal

Proceedings of the National Academy of Sciences of the United States of America, 115(12)

ISSN

0027-8424

Authors

Kurup, Naina
Li, Yunbo
Goncharov, Alexandr
et al.

Publication Date

2018-03-20

DOI

10.1073/pnas.1721930115

Peer reviewed

Intermediate filament accumulation can stabilize microtubules in *Caenorhabditis elegans* motor neurons

Naina Kurup[a], Yunbo Li[a], Alexandr Goncharov[a], and Yishi Jin[a,b,1]

[a]Neurobiology Section, Division of Biological Sciences, University of California, San Diego, La Jolla, CA 92093; and [b]Department of Cellular and Molecular Medicine, University of California, San Diego, La Jolla, CA 92093

Edited by H. Robert Horvitz, Massachusetts Institute of Technology, Cambridge, MA, and approved February 11, 2018 (received for review December 21, 2017)

Neural circuits utilize a coordinated cellular machinery to form and eliminate synaptic connections, with the neuronal cytoskeleton playing a prominent role. During larval development of *Caenorhabditis elegans*, synapses of motor neurons are stereotypically rewired through a process facilitated by dynamic microtubules (MTs). Through a genetic suppressor screen on mutant animals that fail to rewire synapses, and in combination with live imaging and ultrastructural studies, we find that intermediate filaments (IFs) stabilize MTs to prevent synapse rewiring. Genetic ablation of IFs or pharmacological disruption of IF networks restores MT growth and rescues synapse rewiring defects in the mutant animals, indicating that IF accumulation directly alters MT stability. Our work sheds light on the impact of IFs on MT dynamics and axonal transport, which is relevant to the mechanistic understanding of several human motor neuron diseases characterized by IF accumulation in axonal swellings.

microtubules | intermediate filaments | synapses | *C. elegans* | neurons

A robust cytoskeletal network is essential to many aspects of neuronal function, including axon outgrowth, guidance, and maintenance, as well as synapse formation and plasticity (1–3). Intermediate filaments (IFs) are one such cytoskeletal polymer and include different classes that are expressed in a variety of tissues. Neurofilaments (NFs) are a specific IF class expressed in neurons that provide structural support for the establishment of axon caliber in large-diameter myelinated axons (3, 4). Overexpression of NFs in some mouse models has linked NF accumulation to motor neuron death, with impairment of axonal transport thought to be a precursor to neuron degeneration (5–7). Changes in NF levels have also been associated with neuropsychiatric disorders such as bipolar disorder and schizophrenia, although whether NFs alter circuit activity remains unknown (8). The complexity in subunit composition and the variety of posttranslational modifications associated with NFs suggest potential roles for these filaments in neuronal functions outside axon-caliber maintenance (9). For example, several studies have shown a requirement for microtubule (MT) motors in mediating IF motility and report a close association between IFs and MTs during MT assembly (10–12), supporting a mechanistic interaction between the two cytoskeletal networks.

In this study, we describe a role for IF assembly in promoting MT stabilization in *Caenorhabditis elegans*, a genetically tractable animal model extensively used to examine neuronal cytoskeletal architecture (13, 14). A comprehensive comparison of the *C. elegans* connectome in larvae and adults revealed a striking switch in motor neuron connectivity during larval development, independent of axon outgrowth or retraction (15–17). We previously found that an up-regulation in the number of dynamic MTs was required for synaptic vesicle transport during motor neuron synapse rewiring (18). Here, we show that IFs prevent synapse rewiring by hyperstabilizing neuronal MTs in mutant animals with defective synapse rewiring. Our results reveal an unexpected regulatory role for IFs in neurons, furthering our understanding of the complex relationship between various cytoskeletal elements in vivo.

Results

Identification of IF Genes That Regulate Synapse Rewiring. At the end of larval stage 1 (L1), the dorsal D (DD)-type motor neurons rewire their presynaptic connections from the ventral nerve cord (VNC) to the dorsal nerve cord (DNC), concurrent with the birth of ventral D (VD)-type motor neurons, which then form synapses along the VNC (19). We visualized DD-neuron presynaptic terminals using a GFP-tagged synaptobrevin (SNB-1::GFP) reporter (*juIs137*: $P_{flp\text{-}13}$ SNB-1::GFP). In L1 animals, discrete synaptic puncta were present along the ventral neurites (18), but in late larvae and adults, synaptic puncta were only seen along the dorsal neurites (Fig. 1 *A* and *B*). We had previously shown that DD synapse remodeling depends on synergistic interactions between the MT cytoskeleton and the conserved MAPKKK DLK-1 using double-mutant animals with a missense α-tubulin mutation [*tba-1(gf)*] and a loss of function in *dlk-1(0)* that were defective in DD synapse rewiring (18). Adult *tba-1(gf) dlk-1(0)* animals retained synaptic puncta along the VNC, with little to no synapses along the DNC (Fig. 1 *A* and *B*), resulting from a loss of dynamic MTs that impaired synaptic vesicle transport during rewiring (18).

To identify regulators of MT dynamics during synapse rewiring, we screened for mutants that suppressed synapse rewiring defects in *tba-1(gf) dlk-1(0)* animals (18, 20). We identified two independent alleles (*ju982* and *ju963*) of a *C. elegans* IF homolog, *ifp-1* (Fig. S1*A*). IFP-1 contains a conserved rod domain and a C-terminal lamin tail domain and shares 31% sequence identity with human NF α-internexin (21, 22) (Fig. S1*A*). *ju982* caused a conserved leucine 363 to phenylalanine change in the rod domain, while *ju963* changed proline 443 to serine adjacent

Significance

A principal component of the nerve cell is its cytoskeleton—a network of actin, tubulin, and intermediate filament polymers that maintains cell structure, directs cell growth, and transport of cargo. Here, we show that intermediate filaments can alter the dynamics of microtubules to affect developmental synapse remodeling in *Caenorhabditis elegans*. Accumulation of intermediate filaments is concurrent with hyperstablization of microtubules, which in turn prevents synaptic vesicle transport during rewiring. Our results identify a regulatory role for intermediate filaments in neurons in vivo, providing insight into the mechanisms behind neurological disorders such as ALS, where patients often present with accumulations of intermediate filaments in dying nerve cells.

Author contributions: N.K. and Y.J. designed research; N.K., Y.L., and A.G. performed research; N.K., Y.L., A.G., and Y.J. analyzed data; and N.K. and Y.J. wrote the paper.

The authors declare no conflict of interest.

This article is a PNAS Direct Submission.

[1]To whom correspondence should be addressed. Email: yijin@ucsd.edu.

This article contains supporting information online at www.pnas.org/lookup/suppl/doi:10.1073/pnas.1721930115/-/DCSupplemental.

Published online March 6, 2018.

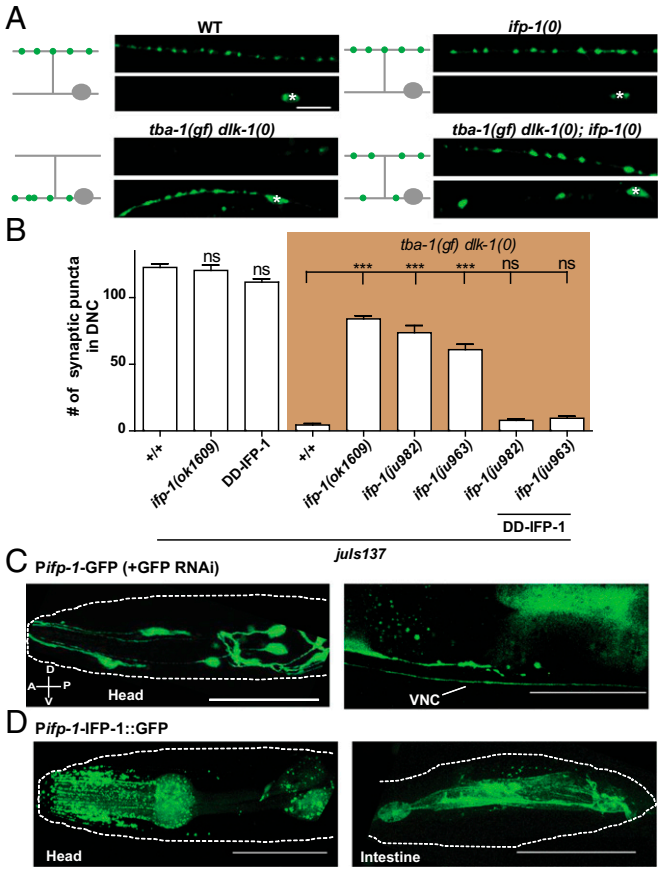

Fig. 1. Loss of *ifp-1* suppresses synapse remodeling defects in *tba-1(gf) dlk-1 (0)*. (*A*) Representative images of DD synapses along the VNC and DNC using P_{flp-13}-SNB-1::GFP (*juIs137*) in adult animals. Schematics of DD neuron (gray) with location of presynaptic vesicles (green) are shown *Left* of each fluorescent image. White asterisks denote DD neuron cell bodies. (Scale bar: 10 μm.) (*B*) Quantification of synaptic puncta in the DNC of adult animals. Data are mean ± SEM; $n > 10$ animals per genotype. DD-IFP-1 denotes extrachromosomal copies of IFP-1(cDNA) expressed in DD neurons under the *flp-13* promoter. Statistics: one-way ANOVA followed by Tukey's posttest; $***P < 0.001$; ns, not significant. (*C*) GFP-RNAi treatment of worms expressing *ifp-1* promoter-driven GFP (P_{ifp-1}-GFP) revealed expression in head neurons and the VNC. (Scale bars: 50 μm.) (*D*) Expression pattern of IFP-1 protein in the head and intestine of WT worms using a C-terminal GFP-tagged IFP-1 expressed under its own promoter. (Scale bars: 50 μm.) See also Fig. S1.

to the rod domain (Fig. S1*A*). Both alleles restored synapses to the dorsal neurite in *tba-1(gf) dlk-1(0)*. A null mutation, *ifp-1(ok1609)* [hereafter denoted *ifp-1(0)*], that removes most of the rod domain and causes a premature stop showed stronger suppression of the synaptic defects of *tba-1(gf) dlk-1(0)* than either *ju982* or *ju963*, suggesting that they were hypomorphic alleles of *ifp-1* (Fig. 1 *A* and *B*). Transgenic overexpression of wild-type IFP-1 specifically in the DD neurons of *tba-1(gf) dlk-1(0); ifp-1(ju982)* and *tba-1(gf) dlk-1(0); ifp-1(ju963)* animals restored the synapse rewiring defects seen in *tba-1(gf) dlk-1(0)* alone (Fig. 1*B*). These results indicated that loss of function in *ifp-1* suppresses *tba-1(gf) dlk-1(0)* phenotypes, and that *ifp-1* acts cell autonomously to regulate DD synapse rewiring. *ifp-1* loss-of-function mutants alone displayed normal synapses, and overexpression of IFP-1 in wild-type animals also did not have an effect on the number of synapses of DD neurons (Fig. 1 *A* and *B*), suggesting that the effect of *ifp-1* on synapse formation was dependent on *tba-1(gf) dlk-1(0)*.

We next characterized IF expression in wild-type and *tba-1(gf) dlk-1(0)* animals. Using a transcriptional GFP reporter (driven by 1 kb upstream of the transcription start site of *ifp-1*), we found that IFP-1 was strongly expressed in the intestine and pharynx, as previously reported (23) (Fig. S1*B*). Low levels of neuronal expression might have been obscured by robust nonneuronal expression. To test this, we used RNAi to reduce the GFP signal in nonneuronal cells, since neurons in *C. elegans* are refractory to systemic RNAi (24). In P*ifp-1-GFP* transgenic animals with dampened intestinal and pharyngeal GFP expression, we observed weak GFP expression in the VNC and some head neurons, which colocalized with a synaptic marker expressed in D neurons (Fig. 1*C* and Fig. S1*C*). We then examined IFP-1 protein expression by generating extrachromosomal transgenic animals expressing GFP fused to the C terminus of genomic IFP-1. We verified that the fusion of GFP did not alter IFP-1 function, based on the rescue of behavioral suppression of *tba-1(gf) dlk-1(0); ifp-1(0)* animals by addition of the transgene (Fig. S1*D*). In wild-type animals, IFP-1::GFP localized to filaments and puncta in the head, pharynx, and intestine in adult animals (Fig. 1*D*). In contrast, expression of IFP-1(L363F)::GFP, mimicking *ifp-1(ju982)*, showed a near complete loss of filamentous expression (Fig. S1*E*). In *tba-1(gf) dlk-1(0)* animals, we observed an increase in IFP-1::GFP filament intensity in the intestine, while the IFP-1::GFP puncta in the head appeared to have been reduced (Fig. S1*F*).

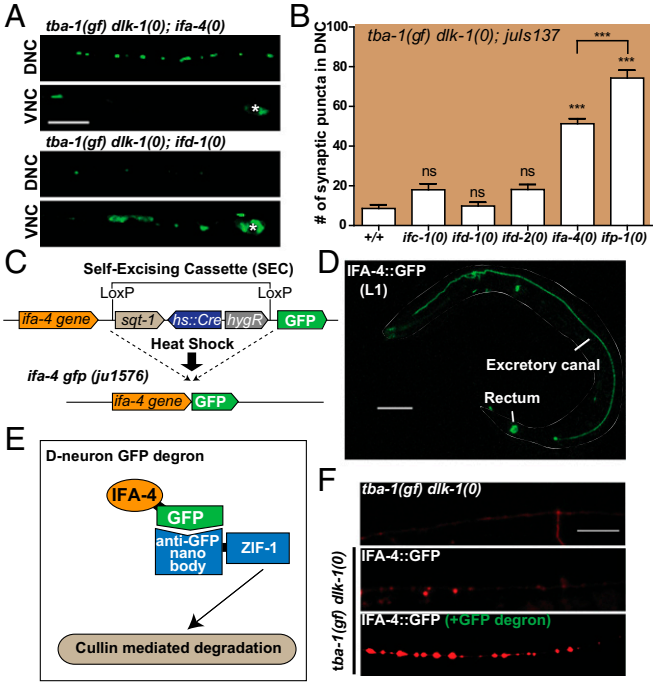

Fig. 2. *ifa-4(0)* also suppresses DD synapse remodeling defects in *tba-1(gf) dlk-1(0)*. (*A*) Representative images of DD synapses in adult animals (*juIs137*). White asterisks denote DD neuron cell bodies. (Scale bar: 10 μm.) (*B*) Quantification of synaptic puncta in the DNC of adult animals. Data are mean ± SEM; $n > 10$ animals per genotype. Statistics: one-way ANOVA followed by Tukey's posttest; $***P < 0.001$; ns, not significant. (*C*) Schematic of CRISPR-Cas9–mediated knockin of GFP at 3′ end of *ifa-4* gene. After homologous recombination of the repair plasmid into the genomic locus, the self-excising cassette is excised following heat shock at 37 °C for 1 h to drive the expression of Cre recombinase. (*D*) Representative image of a wild-type L1 animal expressing endogenous GFP-tagged IFA-4 in the excretory canal and rectum. (Scale bar: 10 μm.) (*E*) Schematic of GFP-degron system targeting IFA-4::GFP in D neurons for cullin-mediated degradation. (*F*) Representative images of the dorsal neurites of adult animals expressing P_{unc-25}-mCherry::RAB-3. (Scale bar: 10 μm.) See also Fig. S2.

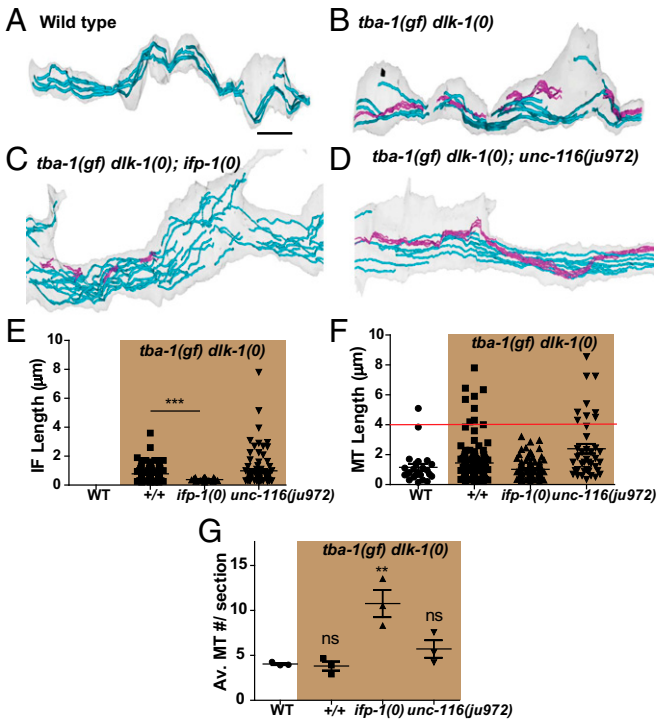

Fig. 3. IFs are present in DD neurons of *tba-1(gf) dlk-1(0)* animals. (*A–D*) Serial reconstruction of EM images from ∼8 µm of the ventral processes of DD neurons in (*A*) WT, (*B*) *tba-1(gf) dlk-1(0)*, (*C*) *tba-1(gf) dlk-1(0); ifp-1(0)*, and (*D*) *tba-1(gf) dlk-1(0); unc-116(ju972)* animals. (Scale bar: 1 µm.) IFs are represented in purple and MTs in blue; the black spot in *B* represents an active zone. (*E*) IF length in the ventral neurite of DD neurons. Data are mean ± SEM. Statistics: Mann–Whitney *U* test; ***$P < 0.001$. Numbers of IFs: 0 for WT, 40 for *tba-1(gf) dlk-1(0)* (■), 20 for *tba-1(gf) dlk-1(0); ifp-1(0)* (▲), and 79 for *tba-1(gf) dlk-1(0); unc-116(ju972)* (▼). (*F*) MT length in the ventral neurite of DD neurons. Data are mean ± SEM. Red line delineates MTs >4 µm in length. Numbers of MTs: 24 for WT (●), 22 for *tba-1(gf) dlk-1(0)* (■), 102 for *tba-1(gf) dlk-1(0); ifp-1(0)* (▲), and 19 for *tba-1(gf) dlk-1(0); unc-116(ju972)* (▼). (*G*) Number of MTs per section in the ventral neurite of various genotypes (each data point represents the mean number of MTs per 50-nm section in 2-µm regions of the axon; symbols as described in *E* and *F*). A total of 120 cross-sections in random order from each strain were analyzed to correlate with actual number of MTs, irrespective of the length of the MTs. Statistics: one-way ANOVA; **$P < 0.001$; ns, not significant. See also Fig. S3 and Movies S1–S4 for full reconstructions of DD neurites.

The *C. elegans* genome encodes 11 cytoplasmic IF homologs, at least 5 of which are essential for development, as null mutants exhibit embryonic or larval lethality (23, 25–28) (Fig. S2*A*). To test whether IFs other than *ifp-1* played a role in DD synapse rewiring, we crossed mutants of the nonessential IFs to *tba-1(gf) dlk-1(0)* double-mutant animals. We counted the number of DNC synapses in *tba-1(gf) dlk-1(0)* adult animals and found that loss of IFA-4 [*ifa-4(0)*] also restored DNC synapses, although to a lesser extent than *ifp-1(0)* (Fig. 2 *A* and *B*). Additionally, *ifp-1(0) ifa-4(0)* animals reduced the number of DNC synapses, suggesting that *ifp-1* acts in concert with other cytoplasmic IFs in wild-type animals to regulate synapse formation (Fig. S2*B*). However, the brood size of *tba-1(gf) dlk-1(0); ifp-1(0) ifa-4(0)* animals was very low, which prevented an accurate analysis of synapse remodeling defects in the quadruple-mutant animals.

To examine endogenous IFA-4 expression, we inserted GFP at the C terminus of IFA-4 using CRISPR-Cas9–mediated genome engineering (Fig. 2*C*) (29). We observed strong expression of IFA-4::GFP (*ju1576*) predominantly in the excretory cells and rectum of young larvae (Fig. 2*D*). In gravid adults, IFA-4::GFP was expressed at the pharyngeal–intestinal valve and formed a network within the uterus (Fig. S2 *B* and *C*). The expression pattern of IFA-4::GFP was largely unaffected by *tba-1(gf) dlk-1(0)*, and we could not detect neuronal expression of IFA-4 protein in either wild-type or *tba-1(gf) dlk-1(0)* animals by live imaging (Fig. 2*D* and Fig. S2 *C* and *D*). However, IFA-4 transcripts were detected in GABAergic D neurons in previous microarray analyses (30). To test that even low expression levels of IFs in D neurons of *tba-1(gf) dlk-1(0)* animals resulted in defective synapse rewiring, we next took advantage of a recently developed GFP-degron system, which enabled the targeted depletion of GFP-tagged proteins in a cell-type specific manner (31, 32). We expressed a transgene containing a nanobody against GFP fused to ZIF-1 specifically in the GABAergic D neurons. Since ZIF-1 targets proteins for cullin-dependent degradation, any GFP-tagged protein in the D neurons would be degraded in animals expressing the transgene while their function remained intact in the rest of the animal (Fig. 2*E*) (31, 32). We confirmed the efficacy of this strategy by visibly knocking down SNB-1::GFP expressed from *juIs137* marker, while a coinjection marker expressing GFP in the AFD neurons was unaffected (Fig. S2*E*). To observe the effects of depleting IFA-4::GFP on DD remodeling, we used *tba-1(gf) dlk-1(0)* animals expressing mCherry::RAB-3 in the D neurons (Fig. 2*F*). Depletion of IFA-4::GFP in the D neurons of *tba-1(gf) dlk-1(0)* animals led to the appearance of mCherry::RAB-3 puncta along the DNC, consistent with the suppression of synapse remodeling defects in *tba-1(gf) dlk-1(0)* by *ifa-4(0)* (Fig. 2*F* and Fig. S2*F*). Together with the loss of synapses along the DNC in *tba-1(gf) dlk-1(0); ifp-1(0)* animals by the overexpression of IFP-1 specifically in the DD neurons

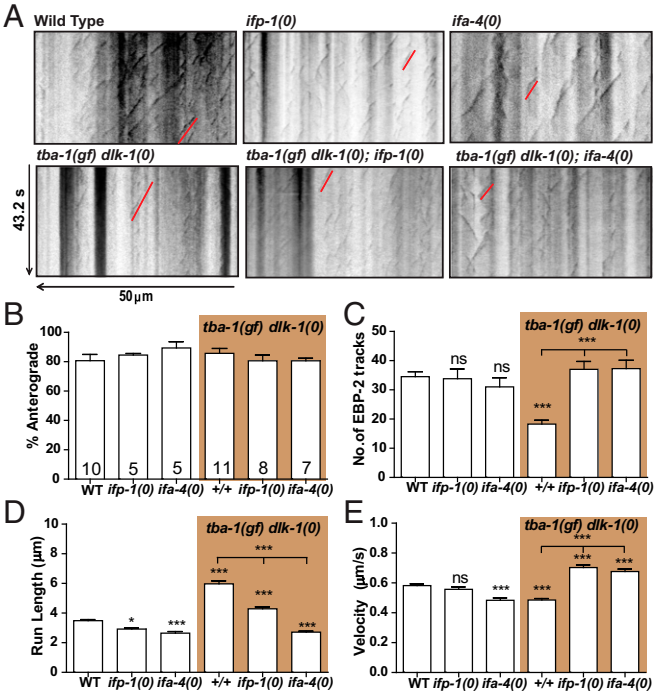

Fig. 4. Loss of IFs promotes MT dynamics in *tba-1(gf) dlk-1(0)* animals. (*A*) Representative kymographs of MT dynamics in adult animals. The *x* axis is distance imaged to generate the kymograph (measured from the cell body), and the *y* axis is duration of imaging. Red lines indicate a single EBP-2::GFP track moving in the anterograde direction. (*B–E*) Quantification of (*B*) direction, (*C*) number, (*D*) run length, and (*E*) velocity of EBP-2::GFP tracks. Data are mean ± SEM; number of animals is shown on *B*. Statistics: one-way ANOVA followed by Tukey's posttest; *$P < 0.05$, ***$P < 0.0001$; ns, not significant.

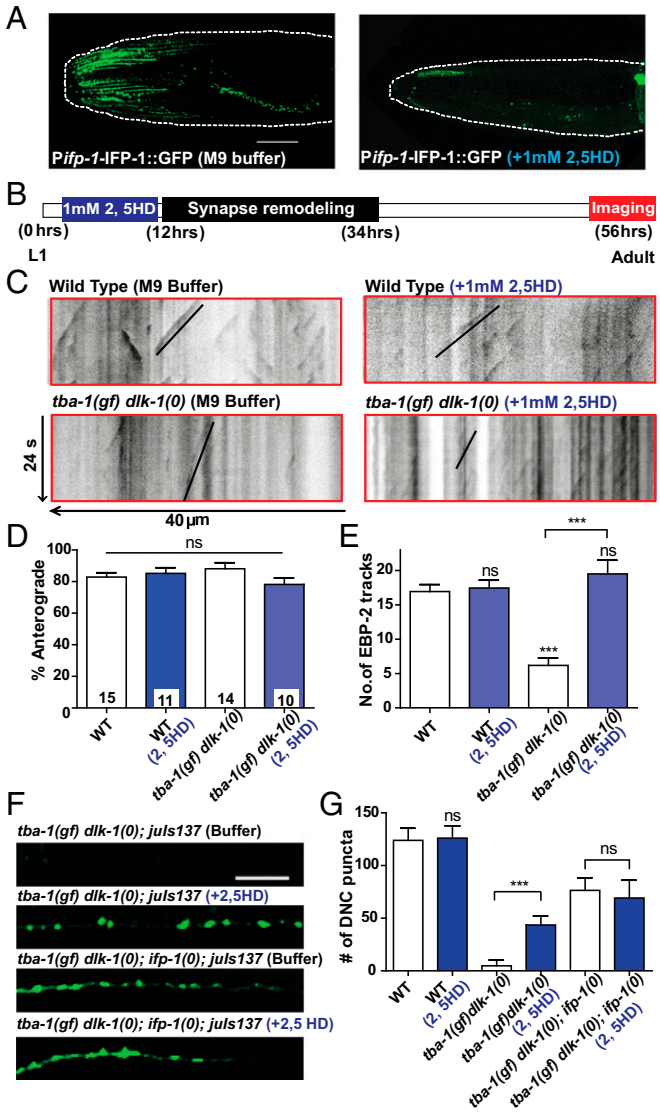

Fig. 5. Acute treatment with 2,5-HD restores MT dynamics and synapse rewiring in *tba-1(gf) dlk-1(0)* animals. (*A*) Expression levels of IFP-1 protein fused to GFP after chronic treatment with 1 mM 2,5-HD or buffer control (M9). Animals were grown in drug-containing plates from embryo to adulthood and imaged at day 1 adult stage. (Scale bar: 20 µm.) (*B*) Representation of acute drug treatment and imaging protocol for MT dynamics and synapse rewiring. (*C*) Representative kymographs of MT dynamics in drug- and buffer control-treated adult animals. Black lines indicate a single EBP-2::GFP track. (*D* and *E*) Quantification of (*D*) direction of movement and (*E*) number of EBP-2::GFP tracks. Data are mean ± SEM; number of animals is shown on *D*. Statistics: one-way ANOVA followed by Tukey's posttest; ***$P < 0.001$; ns, not significant. (*F*) Representative images of DD synapses along the DNC [$P_{flp\text{-}13}$-SNB-1::GFP (*juIs137*)] in adult animals. (Scale bar: 10 µm.) (*G*) Quantification of synaptic puncta in the DNC of adult animals. Data are mean ± SEM; $n > 10$ animals per genotype. Statistics: one-way ANOVA followed by Tukey's posttest; ***$P < 0.001$; ns, not significant. See also Fig. S4.

(Fig. 1*C*), we conclude that an increase in neuronal expression of IFs suppressed synapse rewiring.

IFs Stabilize MTs in DD Motor Neurons. To understand how IF assembly was altered in the DD neurons of *tba-1(gf) dlk-1(0)* animals, we made reconstructions of serial section electron microscopy (EM) images of ∼8 µm of the ventral DD neurite (Fig. 3 *A*–*D* and Fig. S3). We defined IFs as ∼10-nm-diameter continuous filaments along the reconstructed neurites (*SI Materials and Methods*). While we did not detect IFs in the ventral neurite of wild-type DD neurons, we found numerous long IFs in *tba-1(gf) dlk-1(0)* animals (Fig. 3 *A* and *B*). As a control, we also analyzed reconstructed DD neurites in *tba-1(gf) dlk-1(0); unc-116(ju972)* animals, which carried an additional kinesin-1 mutation that suppressed the synapse rewiring defects of *tba-1(gf) dlk-1(0)* without altering MT dynamics (18). *tba-1(gf) dlk-1(0); unc-116(ju972)* animals retained the long IFs seen in *tba-1(gf) dlk-1(0)* animals (Fig. 3 *D* and *E*). In contrast, *tba-1(gf) dlk-1(0); ifp-1(0)* triple-mutant animals had a few fragmented IFs that were significantly shorter than those of *tba-1(gf) dlk-1(0)* animals (Fig. 3 *C* and *E*). Compared with wild-type animals, *tba-1(gf) dlk-1(0)* animals had an additional population of MTs >4 µm in length (Fig. 3 *A*, *B*, and *F*). This population of long MTs was observed in *tba-1(gf) dlk-1(0); unc-116(ju972)* animals, but not in *tba-1(gf) dlk-1(0); ifp-1(0)* triple mutants (Fig. 3 *C*, *D*, and *F*). Additionally, micrographs from *tba-1(gf) dlk-1(0); ifp-1(0)* animals also contained more MTs per section, on average, than both wild-type and *tba-1(gf) dlk-1(0)* animals (Fig. 3*G*). Together, these observations suggested that loss of IFs in *tba-1(gf) dlk-1(0)* animals resulted in a shift from prolonged MT growth to shorter, more numerous MTs.

As the presence of IFs correlated with the presence of longer MTs, we hypothesized that IFs could play a role in modulating MT dynamics. To test this hypothesis, we assayed MT plus-end dynamics in wild-type and *tba-1(gf) dlk-1(0)* animals, as well as *ifp-1(0)* and *ifa-4(0)* animals in the wild-type and *tba-1(gf) dlk-1(0)* backgrounds. We imaged the MT plus-end binding protein EBP-2 tagged to GFP expressed in the D motor neurons and analyzed growing MTs depicted by the appearance of tracks on kymographs (18) (Fig. 4*A*). We performed imaging of MT dynamics in adult animals since the changes we observed during synapse rewiring in L1 were maintained in adult animals (18). Most MT growth was in the anterograde direction in both wild-type and mutant animals (Fig. 4 *A* and *B*). As previously reported (18), *tba-1(gf) dlk-1(0)* animals had a severe reduction in the number of dynamic MTs and a corresponding increase in MT run length and decrease in MT velocity compared with wild-type animals (Fig. 4 *A* and *C*–*E*). *ifp-1(0)* and *ifa-4(0)* single mutants displayed a reduction in MT run length and velocity compared with wild-type animals, but the number of dynamic MTs was unchanged (Fig. 4 *A* and *C*–*E*). Strikingly, both *ifp-1(0)* and *ifa-4(0)* reversed the impairment in MT dynamics in *tba-1(gf) dlk-1(0)* animals (Fig. 4 *A* and *C*–*E*). There was an increase in the number of dynamic MTs in the triple-mutant animals, along with a reduction in run length and increase in MT growth velocity (Fig. 4 *A* and *C*–*E*). This change in MT dynamics was indicative of a transition from a more stable state in *tba-1(gf) dlk-1(0)* animals to a more dynamic state in the triple-mutant animals. Together with the ultrastructural observation of IFs in *tba-1(gf) dlk-1(0)* animals, these data support a role for IFs in stabilizing MTs in DD neurons.

Pharmacological Destabilization of IFs Restores MT Dynamics and Synapse Rewiring. Since we found that loss of IFs in *tba-1(gf) dlk-1(0)* animals could restore MT dynamics and promote synapse rewiring, we next wanted to test if pharmacologically manipulating IF assembly would result in a similar phenotype. 2,5-Hexanedione (2,5-HD) is a metabolite of the industrial solvent hexane that causes IF disruption upon application to cultured mammalian cells and alters NF interaction with MTs in mammalian axons, although the precise mechanism of 2,5-HD action is unclear (33–35). We first characterized the effects of 2,5-HD exposure on *C. elegans* IF assembly using IFP-1::GFP. Chronic exposure of wild-type *C. elegans* to 2,5-HD at concentrations greater than 1 mM resulted in reduced brood size and significant developmental delays or even embryonic lethality (Fig. S4 *A* and *B*), presumably because of the disruption of

essential IF networks in the intestine and epidermis (26, 27). Animals grown on 1 mM 2,5-HD were superficially wild-type in development and brood size (Fig. S4 *A* and *B*). Under this condition, 2,5-HD caused a strong reduction of IFP-1::GFP expression in the head, but IFP-1::GFP in the intestine appeared to aggregate (Fig. 5*A* and Fig. S4*B*).

We then tested whether this change in IF assembly could alter MT dynamics, by treating wild-type and *tba-1(gf) dlk-1(0)* L1 animals with 1 mM 2,5-HD, acutely for ∼9 h before the onset of synapse rewiring (Fig. 5*B*). We found that there was no change in the number or direction of growth of dynamic MTs in wild-type animals after the acute 2,5-HD treatment, consistent with wild-type DD neurons lacking detectable IFs (Fig. 5 *C*–*E*). Interestingly, in *tba-1(gf) dlk-1(0)* animals, acute 2,5-HD treatment caused a significant increase in MT dynamics, while the overall direction of MT growth was unchanged (Fig. 5 *C*–*E*). We also monitored synapse rewiring after acute treatment of L1 larvae with 1 mM 2,5-HD (Fig. 5 *F* and *G*). Acute 2,5-HD treatment did not alter synapse rewiring in wild-type or *tba-1(gf) dlk-1(0); ifp-1(0)* animals (Fig. 5 *F* and *G*). However, there was a significant increase in the number of synaptic puncta successfully reaching the dorsal neurite of adult *tba-1(gf) dlk-1(0)* animals following acute 2,5-HD treatment, resulting in a partial rescue of the synapse rewiring defect (Fig. 5 *F* and *G*). Together, these results suggest that the presence of IFs was sufficient to shift the balance from dynamic to stable MTs to antagonize synapse rewiring in *C. elegans*.

Discussion

Actin, MTs, and IFs constitute the three major cytoskeletal elements in most eukaryotic cells, and their coordinated interactions have been the subject of intense study for decades. The importance of IF–MT interactions in maintaining the cellular IF network was first demonstrated several years ago, when treatment of BHK-21 cells with colchicine to remove MTs resulted in IF aggregation as a juxtanuclear cap (36). Here, we focus on IF–MT interactions in neuronal development, using *C. elegans* as a model. The synapse rewiring defects in *tba-1(gf) dlk-1(0)* double mutants are a result of hyperstable MTs, and loss of function in IF genes *ifp-1* and *ifa-4* restored normal synapse rewiring in this background. We further characterized IF–MT interactions in living animals, revealing an underappreciated regulatory function for neuronal IFs in modulating MT dynamics in vivo. The functional significance of a bidirectional interaction between IF and MT networks is particularly relevant in neurodegenerative disease conditions like giant axonal neuropathy, ALS, and Charcot-Marie-Tooth disease, where toxic assemblies of IFs in neurons correlate with a fatal loss of motor and sensory function (37, 38). In wild-type DD motor neurons, absence of IFs does not alter circuit rewiring to a large extent, suggesting that regulation of MT dynamics by IFs depends on special conditions. Overexpression of IFP-1 also does not cause any defects in wild-type animals. These data suggest that IF protein expression is tightly regulated in wild-type neurons in the absence of additional perturbations.

Several observations are conducive to the idea that axonal MT stability is directly linked to IF levels. IFs are down-regulated following axonal injury in both the central and peripheral nervous systems (39, 40), which correlates with increased MT destabilization immediately after lesion in a variety of models (14, 41). IF up-regulation is a hallmark of activated astrocytes, and both IF and MT depolymerization can alter the directional motility of vesicles in rat astrocytes (42). Recently, vimentin IFs have also been shown to act as a template for MT stabilization during cell migration in wounded retinal epithelial cells (12). Together with our findings during *C.elegans* synapse rewiring, these results point to a universal role for IF–MT interactions in modulating both IF and MT stability.

The interactions between IF and MT networks have long been thought to occur through a variety of cross-bridging molecules that contain both MT and IF binding domains. During astrocyte migration, the MT-dependent rearrangements of IFs require the tumor suppressor adenomatous polyposis coli (APC) as a cross-bridging molecule to mediate IF–MT interaction (43). Plectin (44) and MAP2/tau (45) have also been implicated as potential IF–MT cross-bridging molecules, but mutant *C. elegans* tau [*ptl-1(0)*] (20) could not phenocopy IF subunit loss in *tba-1(gf) dlk-1(0)* animals. Homologs of APC (*apr-1*) and plectin (*vab-10*) are essential for *C. elegans* embryonic development; future experiments will be necessary to selectively eliminate these genes' function in neurons to elucidate their role in IF–MT interactions. IFs have also been thought to interact with MTs through MT motors like kinesin and dynein (10); however, the kinesin and dynein mutations identified in our suppressor screen had no effect on MT dynamics or composition in *tba-1(gf) dlk-1(0)* animals (Fig. 3 *D* and *E*) (18, 20). Another possible mechanism for IF regulation of MTs involves changes in IF posttranslational modifications like phosphorylation, which control IF interaction with MT-associated proteins (9, 10). However, both *ifp-1* and *ifa-4* lack the KSP repeat motif that is typically phosphorylated in mammalian NFs (9, 10). Further studies are required to understand how IFs and MTs interact during synapse development, and *C.elegans* provides a useful genetic model to dissect the pathways involved in mediating this interaction.

Materials and Methods

C. elegans strains were maintained at 20 to 22 °C on nematode growth medium plates following standard practices. Information on alleles and genotypes of strains and plasmids used for injection is summarized in Tables S1–S3. Additional details of imaging, EM image serial reconstruction, and staging conditions for drug and RNAi treatment are provided in *SI Materials and Methods*. Statistical analysis was performed using GraphPad Prism 5. Details of the statistical analyses performed for each graph are presented in the corresponding figure legends.

ACKNOWLEDGMENTS. We thank A. D. Chisholm, K. McCulloch, N. H. Tang, C. Piggott, K. W. Kim, S. Park, and M. Andrusiak for comments on the manuscript; and other members of the Y.J. laboratory for useful discussions during the course of the study. We thank the Caenorhabditis Genetics Center, which is supported by the National Institutes of Health (NIH) (Grant P40 OD010440), and the Mitani laboratory (Tokyo Women's Medical College) for strains used in this study. Y.J. was an Investigator and A.G. was a Research Associate of the Howard Hughes Medical Institute (HHMI). N.K. was a recipient of the Latham & Watkins Graduate Fellowship. This work was supported by the HHMI and by an NIH grant (NINDS R01 035546, to Y.J.).

1. Conde C, Cáceres A (2009) Microtubule assembly, organization and dynamics in axons and dendrites. *Nat Rev Neurosci* 10:319–332.
2. Dillon C, Goda Y (2005) The actin cytoskeleton: Integrating form and function at the synapse. *Annu Rev Neurosci* 28:25–55.
3. Yuan A, Rao MV, Veeranna, Nixon RA (2017) Neurofilaments and neurofilament proteins in health and disease. *Cold Spring Harb Perspect Biol* 9:a018309.
4. Lee MK, Cleveland DW (1996) Neuronal intermediate filaments. *Annu Rev Neurosci* 19:187–217.
5. Beaulieu JM, Nguyen MD, Julien JP (1999) Late onset of motor neurons in mice overexpressing wild-type peripherin. *J Cell Biol* 147:531–544.
6. Lee MK, Marszalek JR, Cleveland DW (1994) A mutant neurofilament subunit causes massive, selective motor neuron death: Implications for the pathogenesis of human motor neuron disease. *Neuron* 13:975–988.
7. Xu Z, Cork LC, Griffin JW, Cleveland DW (1993) Increased expression of neurofilament subunit NF-L produces morphological alterations that resemble the pathology of human motor neuron disease. *Cell* 73:23–33.
8. Yuan A, Nixon RA (2016) Specialized roles of neurofilament proteins in synapses: Relevance to neuropsychiatric disorders. *Brain Res Bull* 126:334–346.
9. Snider NT, Omary MB (2014) Post-translational modifications of intermediate filament proteins: Mechanisms and functions. *Nat Rev Mol Cell Biol* 15:163–177.
10. Chang L, Goldman RD (2004) Intermediate filaments mediate cytoskeletal crosstalk. *Nat Rev Mol Cell Biol* 5:601–613.
11. Bocquet A, et al. (2009) Neurofilaments bind tubulin and modulate its polymerization. *J Neurosci* 29:11043–11054.
12. Gan Z, et al. (2016) Vimentin intermediate filaments template microtubule networks to enhance persistence in cell polarity and directed migration. *Cell Syst* 3:252–263.e8.

13. Chalfie M, Thomson JN (1982) Structural and functional diversity in the neuronal microtubules of *Caenorhabditis elegans*. *J Cell Biol* 93:15–23.
14. Chisholm AD, Hutter H, Jin Y, Wadsworth WG (2016) The genetics of axon guidance and axon regeneration in *Caenorhabditis elegans*. *Genetics* 204:849–882.
15. White JG, Albertson DG, Anness MAR (1978) Connectivity changes in a class of motoneurone during the development of a nematode. *Nature* 271:764–766.
16. White JG, Southgate E, Thomson JN, Brenner S (1986) The structure of the nervous system of the nematode *Caenorhabditis elegans*. *Philos Trans R Soc Lond B Biol Sci* 314:1–340.
17. Hallam SJ, Jin Y (1998) lin-14 Regulates the timing of synaptic remodelling in *Caenorhabditis elegans*. *Nature* 395:78–82.
18. Kurup N, Yan D, Goncharov A, Jin Y (2015) Dynamic microtubules drive circuit rewiring in the absence of neurite remodeling. *Curr Biol* 25:1594–1605.
19. Kurup N, Jin Y (2015) Neural circuit rewiring: Insights from DD synapse remodeling. *Worm* 5:e1129486.
20. Kurup N, Yan D, Kono K, Jin Y (2017) Differential regulation of polarized synaptic vesicle trafficking and synapse stability in neural circuit rewiring in *Caenorhabditis elegans*. *PLoS Genet* 13:e1006844.
21. Kaplan MP, Chin SS, Fliegner KH, Liem RK (1990) α-Internexin, a novel neuronal intermediate filament protein, precedes the low molecular weight neurofilament protein (NF-L) in the developing rat brain. *J Neurosci* 10:2735–2748.
22. Yuan A, et al. (2006) α-Internexin is structurally and functionally associated with the neurofilament triplet proteins in the mature CNS. *J Neurosci* 26:10006–10019.
23. Karabinos A, Schünemann J, Weber K (2004) Most genes encoding cytoplasmic intermediate filament (IF) proteins of the nematode *Caenorhabditis elegans* are required in late embryogenesis. *Eur J Cell Biol* 83:457–468.
24. Winston WM, Molodowitch C, Hunter CP (2002) Systemic RNAi in *C. elegans* requires the putative transmembrane protein SID-1. *Science* 295:2456–2459.
25. Carberry K, Wiesenfahrt T, Windoffer R, Bossinger O, Leube RE (2009) Intermediate filaments in *Caenorhabditis elegans*. *Cell Motil Cytoskeleton* 66:852–864.
26. Karabinos A, Schmidt H, Harborth J, Schnabel R, Weber K (2001) Essential roles for four cytoplasmic intermediate filament proteins in *Caenorhabditis elegans* development. *Proc Natl Acad Sci USA* 98:7863–7868.
27. Woo WM, Goncharov A, Jin Y, Chisholm AD (2004) Intermediate filaments are required for *C. elegans* epidermal elongation. *Dev Biol* 267:216–229.
28. Zuela N, Gruenbaum Y (2016) Intermediate filaments in Caenorhabditis elegans. *Methods Enzymol* 568:661–679.
29. Dickinson DJ, Ward JD, Reiner DJ, Goldstein B (2013) Engineering the *Caenorhabditis elegans* genome using Cas9-triggered homologous recombination. *Nat Methods* 10:1028–1034.
30. Spencer WC, et al. (2011) A spatial and temporal map of *C. elegans* gene expression. *Genome Res* 21:325–341.
31. Armenti ST, Lohmer LL, Sherwood DR, Nance J (2014) Repurposing an endogenous degradation system for rapid and targeted depletion of *C. elegans* proteins. *Development* 141:4640–4647.
32. Wang S, et al. (2017) A toolkit for GFP-mediated tissue-specific protein degradation in C. elegans. *Development* 144:2694–2701.
33. Durham HD (1987) 2,5-Hexanedione aggregates vimentin-, but not keratin-, intermediate filaments of PtK1 cells. *Cell Biol Int Rep* 11:307–318.
34. Xue C, Shtylla B, Brown A (2015) A stochastic multiscale model that explains the segregation of axonal microtubules and neurofilaments in neurological diseases. *PLoS Comput Biol* 11:e1004406.
35. Llorens J (2013) Toxic neurofilamentous axonopathies–Accumulation of neurofilaments and axonal degeneration. *J Intern Med* 273:478–489.
36. Goldman RD (1971) The role of three cytoplasmic fibers in BHK-21 cell motility. I. Microtubules and the effects of colchicine. *J Cell Biol* 51:752–762.
37. Lariviere RC, Julien JP (2004) Functions of intermediate filaments in neuronal development and disease. *J Neurobiol* 58:131–148.
38. Asbury AK, Gale MK, Cox SC, Baringer JR, Berg BO (1972) Giant axonal neuropathy—A unique case with segmental neurofilamentous masses. *Acta Neuropathol* 20:237–247.
39. Hoffman PN, Pollock SC, Striph GG (1993) Altered gene expression after optic nerve transection: Reduced neurofilament expression as a general expression as a general response to axonal injury. *Exp Neurol* 119:32–36.
40. Hoffman PN, Cleveland DW (1988) Neurofilament and tubulin expression recapitulates the developmental program during axonal regeneration: Induction of a specific beta-tubulin isotype. *Proc Natl Acad Sci USA* 85:4530–4533.
41. Bradke F, Fawcett JW, Spira ME (2012) Assembly of a new growth cone after axotomy: The precursor to axon regeneration. *Nat Rev Neurosci* 13:183–193.
42. Potokar M, et al. (2007) Cytoskeleton and vesicle mobility in astrocytes. *Traffic* 8:12–20.
43. Sakamoto Y, Boëda B, Etienne-Manneville S (2013) APC binds intermediate filaments and is required for their reorganization during cell migration. *J Cell Biol* 200:249–258.
44. Svitkina TM, Verkhovsky AB, Borisy GG (1996) Plectin sidearms mediate interaction of intermediate filaments with microtubules and other components of the cytoskeleton. *J Cell Biol* 135:991–1007.
45. Miyata Y, Hoshi M, Nishida E, Minami Y, Sakai H (1986) Binding of microtubule-associated protein 2 and tau to the intermediate filament reassembled from neurofilament 70-kDa subunit protein. Its regulation by calmodulin. *J Biol Chem* 261:13026–13030.